

## Phase Diagram of Water under an Applied Electric Field

J. L. Aragones,<sup>1,2</sup> L. G. MacDowell,<sup>1</sup> J. I. Siepmann,<sup>2</sup> and C. Vega<sup>1,\*</sup>

<sup>1</sup>*Departamento de Química Física, Facultad de Química, Universidad Complutense de Madrid, 28040, Madrid, Spain*

<sup>2</sup>*Department of Chemistry and Chemical Theory Center, University of Minnesota, Minneapolis, Minnesota 55455, USA*

(Received 21 July 2011; revised manuscript received 27 July 2011; published 3 October 2011)

Simulations are used to investigate for the first time the anisotropy of the dielectric response and the effects of an applied electric field  $\mathbf{E}_{\text{ex}}$  on the phase diagram of water. In the presence of electric fields ice II disappears from the phase diagram. When  $\mathbf{E}_{\text{ex}}$  is applied in the direction perpendicular to the *ac* crystallographic plane the melting temperatures of ices III and V increase whereas that of ice *Ih* is hardly affected. Ice III also disappears as a stable phase when  $\mathbf{E}_{\text{ex}}$  is applied in the direction perpendicular to the *ab* plane.  $\mathbf{E}_{\text{ex}}$  increases by a small amount the critical temperature and reduces slightly the temperature of the maximum density of liquid water. The presence  $\mathbf{E}_{\text{ex}}$  modifies all phase transitions of water but its effect on solid-solid and solid-fluid transitions seems to be more important and different depending on the direction of  $\mathbf{E}_{\text{ex}}$ .

DOI: 10.1103/PhysRevLett.107.155702

PACS numbers: 64.70.-p, 61.20.Ja

Applied electric fields,  $\mathbf{E}_{\text{ex}}$ , modify the properties of all phases of matter but to different extents and, hence, can change the location of phase transitions. The phase diagram of water exhibits a large number of polymorphs. Thus, there is significant interest in exploring the effects of  $\mathbf{E}_{\text{ex}}$  on the properties of water's condensed phases and on its phase diagram. Attempts have been made to determine whether  $\mathbf{E}_{\text{ex}}$  affects the melting point of ice *Ih* [1]. Also, the effects of  $\mathbf{E}_{\text{ex}}$  on the structural properties of liquid water and on gas-to-liquid nucleation rates have been investigated [2,3], while recently it has been shown that  $|\mathbf{E}_{\text{ex}}| \leq 0.3$  V/nm leads to relatively small changes for water's vapor-liquid phase envelope [4]. Theoretically, it is understood that  $\mathbf{E}_{\text{ex}}$  stabilizes phases with high dielectric constant. Since solid phases are generally anisotropic, the relative stabilization will depend on the magnitude and on the orientation of  $\mathbf{E}_{\text{ex}}$  with respect to the crystal. However, the dielectric constant has been measured only for a limited set of state points for some solid phases of water, either experimentally [5] or from simulation [6,7] and very little is known as to the anisotropy of its dielectric response [8].

Here, we present a simulation study of the dielectric constant tensor for several solid phases and the effects of  $\mathbf{E}_{\text{ex}}$  on the phase diagram of water, described by the non-polarizable TIP4P/2005 model [9]. We show that electric fields exhibit a dramatic effect for boundaries between ordered or disordered phases. Particularly, we find that for  $\mathbf{E}_{\text{ex}} > 0$ , ice II, an ordered phase, is destabilized to the point of completely vanishing from the phase diagram.  $\mathbf{E}_{\text{ex}}$  applied along the axis of smallest dielectric response further washes out ice III from the phase diagram. It should be recognized that a nonpolarizable model with its effective dipole moment,  $\mu_{\text{eff}}$ , cannot quantitatively represent the dielectric properties over a wide range of state points. However, we have shown that the dielectric constants of ices can be reproduced reasonably well when the calculated

polarization factor,  $G_{\text{pol}}$ , for the TIP4P/2005 model is scaled to account for the difference between the accurate average molecular dipole moment,  $\mu_{\text{acc}}$ , in a given phase and  $\mu_{\text{eff}}$  of the model [10,11]. This scaling approach is also used here for the determination of the phase boundaries.

For  $|\mathbf{E}_{\text{ex}}| > 0$ , the dipolar water molecules tend to align with the field direction. For liquid and vapor phases, molecules can reorient without encountering large barriers, but the situation is different for solid phases. Ices can be divided in to proton-ordered (II, VIII ...) and proton-disordered phases (*Ih*, III, V, VI ...). Molecular reorientation is not permitted for proton-ordered phases, whereas the extent of the reorientation depends on the crystalline structure and thermodynamic state for proton-disordered phases. The relaxation times in proton-disordered structures can be very long ( $\mu\text{s}$ ) and for this reason it is necessary to bias the simulations (by introducing Monte Carlo moves that sample efficiently the proton rearrangement) to determine the response of the system under a perturbation such as  $\mathbf{E}_{\text{ex}}$ . We have implemented a rotational loop algorithm [6,12]. Under the presence of a homogeneous static electric field,  $\mathbf{E}$ , changes in the internal energy,  $U = K + V_{\text{inter}}$ , can be written as [13]

$$dU = TdS - pdV + \mathbf{E}d\mathbf{M} + \mu dN, \quad (1)$$

where  $\mathbf{M}$  is the total dipole moment of the system. The value of the electric field  $\mathbf{E}$  is in general different from the applied external field  $\mathbf{E}_{\text{ex}}$  due to the additional field generated by the polarized surface of the cavity [14] which depends on its geometry and the anisotropy of the dielectric constant [11]. Following Alberty [13], let us define  $G_E = G - \mathbf{E} \cdot \mathbf{M}$  and  $H_E = H - \mathbf{E} \cdot \mathbf{M}$  that are related through  $\partial(G_E/T)/\partial(1/T) = H_E$ . Phase transitions at constant  $\mathbf{E}_{\text{ex}}$ ,  $T$  and  $p$  require that both phases have the same  $\mu = G_E/N$ . From a microscopic point of view  $G_E = -kT \ln(Q')$  with  $Q'$ :

$$Q' \propto \int \exp(-\beta(V_{\text{inter}} + pV - \mathbf{M}\mathbf{E}_{\text{ex}} + U_{\text{pol}})) d\mathbf{r}^N dV. \quad (2)$$

When Ewald sums are used (as done in this work)  $V_{\text{inter}}$  includes the real and reciprocal space contributions to the Coulombic energy of the system. The term  $U_{\text{pol}}$  is the interaction energy of the system with the polarized surface [14]. Here we shall assume a spherical sample (formed by many simulation boxes) under conducting periodic boundary conditions so that  $U_{\text{pol}}$  vanishes and  $\mathbf{E}$  and  $\mathbf{E}_{\text{ex}}$  become identical [14]. Differentiating  $G_E$  with respect to  $\mathbf{E}_{\text{ex}}$  yields  $-\langle \mathbf{M} \rangle$ , and its integral allows one to evaluate how  $G_E$  changes under the influence of a field as follows

$$G_E(E_{\text{ex}}) - G_E(0) = - \int_{E=0}^{E_{\text{ex}}} \langle M_{\parallel} \rangle_{N,p,T,E_{\text{ex}}} dE_{\text{ex}}. \quad (3)$$

The integrand of Eq. (3) (i.e., the polarization in the direction of the applied electric field) is easily obtained by performing  $NpT$  simulations at different values of  $\mathbf{E}_{\text{ex}}$ , and  $G_E(0)$  has been determined by Abascal and Vega for the phase diagram of the TIP4P/2005 water model [9]. Once  $G_E(E_{\text{ex}})$  has been computed for a specific reference state of each phase, thermodynamic integration in  $p, T$  space can be used to locate a point where two phases coexist. After that, Gibbs-Duhem integration [15] is used to trace the coexistence line. Simulation details for the solid-phase simulations (constant-stress ensemble, system size, types of moves) follow those described in our previous work [10,11].

The polarization response of liquid water and ice *Ih* to  $\mathbf{E}$  is illustrated in Fig. 1. For  $\mathbf{E} < 0.1$  V/nm, the polarization response is linear for both phases, but the slope is somewhat larger for the liquid phase. For  $\mathbf{E} > 0.1$  V/nm, the polarization response is not linear. Let us define the

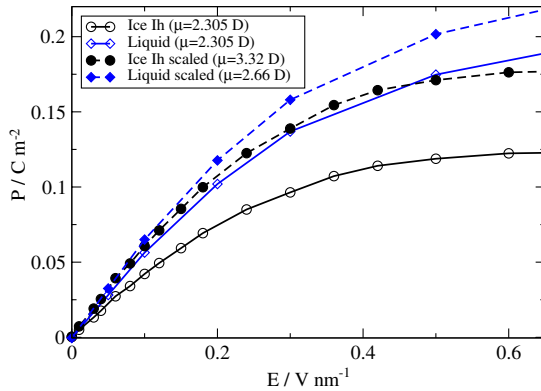


FIG. 1 (color online). Polarization ( $P$ ) as function of  $\mathbf{E}$  for the liquid phase (open diamonds and solid line) and the ice *Ih* phase (open circles and solid line) computed for the TIP4P/2005 model at 250 K and 1 bar. The corresponding values obtained by scaling the magnitude of the molecular dipole moment are indicated by filled symbols and dashed lines. For ice *Ih* the applied field was in the direction perpendicular to the *ac* plane and  $P$  stands for  $P_{\perp ac}$ .

degree of saturation as  $S_M = \langle M \rangle / (N\mu_{\text{eff}})$ . For liquid water values close to unity are obtained for  $S_M$  at high  $\mathbf{E}$  as the molecules are free to orient their dipoles with the field direction. For ice *Ih*, however,  $S_M$  reaches a limit of  $\approx 0.58$  at high  $\mathbf{E}$  because the geometric constraints of the solid structure of ice *Ih* prevent complete saturation.

For small  $\mathbf{E}$ , the polarization of the system  $\mathbf{P} = \mathbf{M}/V$  is related to the field strength through the expression  $\mathbf{P} = \chi\mathbf{E}$ , where  $\chi$  is the susceptibility tensor given by  $\epsilon - \mathbf{I}$  with  $\epsilon$  and  $\mathbf{I}$  being the dielectric constant tensor and the identity matrix [16]. In computer simulations the dielectric constant tensor can be determined either by analyzing the fluctuations of the system dipole [6,10,11,17] or through the polarization response of the system [18]. In this work, we have used the latter method and applied  $\mathbf{E}$  in different crystallographic directions to resolve the anisotropy of the dielectric constant tensor. A comparison with literature data (see Table I) shows good agreement between the two computational approaches.

The dielectric constant tensor exhibits significant anisotropy for ices III, V, and VI. The TIP4P/2005 model under predicts the dielectric constants of liquid and solid phases by about 25%. However, it predicts correctly the polarization factor,  $G_{\text{pol}} = \langle M^2 \rangle / N\mu^2$ , which contains information about the orientational structure of water, and the underestimation of the dielectric constant is due to  $\mu_{\text{eff}} = 2.305$  D for this model being too small. First principles studies indicate that the average dipole moment of water molecules in the condensed phases is  $\approx 2.7$  D for liquid water and  $\approx 3.3$  D for ice *Ih* [19,20]. Thus, the TIP4P/2005 model is capable of predicting qualitatively the effects of  $\mathbf{E}_{\text{ex}}$  on the phase boundaries, but for quantitative predictions a scaling of the dipole moment to an accurate value  $\mu_{\text{acc}}$  is needed.

For  $\mathbf{E}_{\text{ex}} > 0$ ,  $G_E$  is lower than for  $\mathbf{E}_{\text{ex}} = 0$  [see Eq. (3)], and the extent of the reduction is proportional to  $\langle M_{\parallel} \rangle$ . Therefore, when  $\mathbf{E}_{\text{ex}} > 0$ , the phase with higher  $\epsilon$  will become relatively more stable (larger reduction in  $G_E$ ). Since the dielectric constant is a tensor the effect of  $\mathbf{E}_{\text{ex}}$  will depend on its direction with respect to the crystal. For ice *Ih*, the three components are about equal, whereas  $\epsilon$  for the other ice polymorphs is anisotropic (see Table I). To study the effect of  $\mathbf{E}_{\text{ex}}$  on the phase diagram of water, we have chosen to apply  $\mathbf{E}_{\text{ex}}$  in the direction perpendicular to the *ac* plane (i.e.,  $\mathbf{E}_{\text{ex} \perp ac}$ ) for crystalline phases (c.f. caption of Table I for details) because  $\epsilon_{yy}$  is larger than the other components, and this field direction allows for the maximum reduction in  $G_E$  for a given field strength. We assume that one studies a single crystal with a well-defined orientation with respect to the field. For a polycrystalline sample, the orientations of the microcrystals with respect to  $\mathbf{E}_{\text{ex}}$  would be random, i.e., leading to broadening of the melting temperature.

A comparison of the phase diagrams computed for the TIP4P/2005 water model at  $\mathbf{E}_{\text{ex} \perp ac} = 0.3$  V/nm with and

TABLE I. Dielectric constants obtained for the TIP4P/2005 model from equilibrium fluctuations [10] (Fluc) at  $\mathbf{E}_{\text{ex}} = 0$  and from linear response (LR). For ices III and VI the laboratory frame defining  $x$ ,  $y$  and  $z$  is chosen in the direction of the unit cell vectors  $a$ ,  $b$ , and  $c$  [16]. For ices Ih and II,  $x$  and  $z$  are located along  $a$  and  $c$ ;  $y$  is chosen in the direction perpendicular to the  $ac$  plane (ice II was described with an hexagonal unit cell instead of the trigonal one). With this choice of the laboratory frame the susceptibility tensor is diagonal. For ice V, the  $x$  and  $y$  axes are located along the  $a$  and  $b$  vectors and  $z$  is perpendicular to the  $ab$  plane. The subscripts indicate the statistical uncertainty. Using dipole scaling, the  $\epsilon$  values increase by  $(2.66/2.305)^2$  and  $(3.32/2.305)^2$  for the liquid and solid phases, respectively.

phase	$p$	$T$	$\epsilon_{xx}$		$\epsilon_{yy}$		$\epsilon_{zz}$	
			LR	Fluc	LR	Fluc	LR	Fluc
L	1	250	58 <sub>8</sub>	56 <sub>3</sub>	...	...	...	...
Ih	1	243	49 <sub>7</sub>	53 <sub>2</sub>	...	53 <sub>2</sub>	...	53 <sub>2</sub>
II	3016	180	2 <sub>13</sub>	...	...	...	...	...
III	2800	243	75 <sub>10</sub>	80 <sub>15</sub>	77 <sub>9</sub>	84 <sub>11</sub>	4 <sub>8</sub>	15 <sub>5</sub>
V	5300	180	79 <sub>10</sub>	75 <sub>25</sub>	118 <sub>9</sub>	161 <sub>37</sub>	56 <sub>8</sub>	71 <sub>13</sub>
VI	11 000	260	83 <sub>10</sub>	...	...	...	42 <sub>8</sub>	...
VI	11 000	243	...	102 <sub>40</sub>	...	115 <sub>36</sub>	...	41 <sub>10</sub>

without dipole scaling and that in the absence of a field, is shown in Fig. 2. Our choice of field strength is motivated by previous findings indicating that high fields are needed for statistically significant shifts in the phase boundaries [4]. A field strength of 0.3 V/nm significantly exceeds the dielectric breakdown strength of bulk water samples, but is only 3 times larger than the 0.1 V/nm reached recently in microfluidic channels [21]. For the TIP4P/2005 model the electric field removes ice II from the phase diagram and shifts the melting temperature of ice Ih down by about 10 K to lower temperatures. It is more interesting to analyze the behavior of TIP4P/2005 when using dipole scaling, since then dielectric constants of condensed phases are reproduced reasonably well [10] so that the predictions of the model should be closer to what is expected to occur in the

experiment. With the dipole scaling ice II again disappears from the phase diagram, ice V increases significantly its stability range, the melting point of ices III and V increase by about 15 K and the melting point of ice Ih is hardly affected by the field. This last prediction is consistent with experimental results at lower fields [1]. The key to understand these changes is to realize that phases with high dielectric constant increase their stability at the expense of phases with lower dielectric constant. The melting line of ice Ih at  $\mathbf{E}_{\text{ex}\perp\text{ac}} = 0.3$  V/nm closely traces that found without a field. The reason is that the scaled polarization curves are quite similar for liquid water and ice Ih up to this field strength (see Fig. 1).

The principal effect of  $\mathbf{E}_{\text{ex}\perp\text{ac}}$  is the displacement of the phase boundaries. The slopes of the phase transitions are not much affected by the field. The only exception is the change of slope of the V–VI transition from positive to negative values. This is a consequence of the lower enthalpy of ice V with respect to ice VI in the presence of the field. Another interesting result is obtained when the  $\mathbf{E}_{\text{ex}}$  is applied perpendicular to the  $ab$  plane (Fig. 2). Now besides ice II, ice III also disappears from the phase diagram because of its very small value of  $\epsilon_{zz}$  value.

Let us now focus on the effect of the field on fluid phases. Here, we have also studied the influence of  $\mathbf{E}_{\text{ex}} = 0.3$  V/nm on the vapor-liquid coexistence curve (VLCC) for the TIP4P/2005 model (without dipole scaling). Gibbs ensemble Monte Carlo [22] simulations were carried out to compute the VLCC, and the simulation and analysis details follow those used previously for the TIP4P model [4]. The VLCC exhibits a small increase in liquid density and small decrease in vapor density in the presence of the field (see Fig. 3). The critical temperature is increased from  $643 \pm 1$  to  $648 \pm 1$  K, the critical density is reduced from  $0.309 \pm 0.004$  to  $0.307 \pm 0.003$  g/cm<sup>3</sup>, and the normal boiling temperature is increased from  $398.5 \pm 0.6$  to

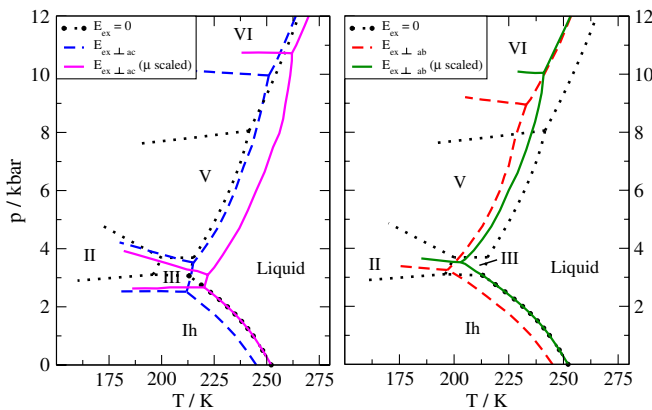


FIG. 2 (color online). Phase diagram for the TIP4P/2005 water model. Dotted black, dashed blue, solid magenta, dashed red and solid green lines indicate the phase boundaries for  $\mathbf{E}_{\text{ex}} = 0$ ,  $\mathbf{E}_{\text{ex}\perp\text{ac}} = 0.3$  V/nm with  $\mu_{\text{eff}}$ ,  $\mathbf{E}_{\text{ex}\perp\text{ac}} = 0.3$  V/nm and dipole scaling using 2.66 and 3.32 D for the liquid and crystalline phases,  $\mathbf{E}_{\text{ex}\perp\text{ab}} = 0.3$  V/nm with  $\mu_{\text{eff}}$  and  $\mathbf{E}_{\text{ex}\perp\text{ab}} = 0.3$  V/nm and dipole scaling, respectively.

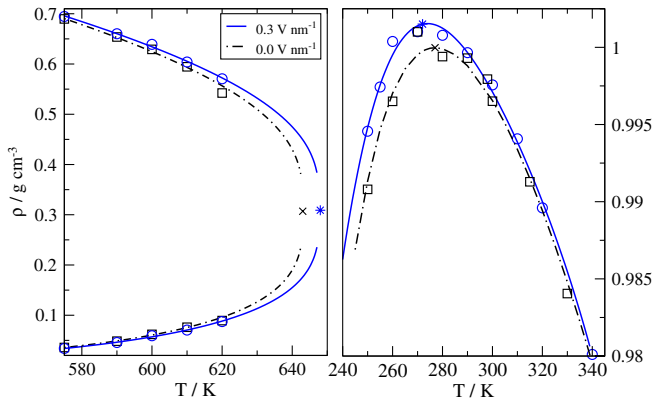


FIG. 3 (color online). Vapor-liquid coexistence curve (left) and temperature dependence of the liquid density (right) for the TIP4P/2005 model at  $\mathbf{E}_{\text{ex}} = 0.3 \text{ V/nm}$  (blue circles and solid lines) and in the absence of a field (black squares and dashed lines). The blue stars and black crosses denote the corresponding critical points and temperatures of maximum density.

$399.2 \pm 0.7 \text{ K}$ . The relatively small extent of these shifts agrees well with results for the TIP4P model [4]. One of the fingerprint properties of water is the existence of a density maximum occurring at  $T_{\text{md}} = 277 \text{ K}$  (at 1 bar). Here, we find that  $T_{\text{md}}$  shifts downward to  $272 \text{ K}$  for  $\mathbf{E}_{\text{ex}} = 0.3 \text{ V/nm}$  (see Fig. 3). The preferential alignment of the water molecules with the field direction leads to a slight decrease in the tetrahedral order [4] and an increase in the density especially for  $T < 300 \text{ K}$ .

In conclusion, efficient simulation algorithms have been used to investigate the effect of  $\mathbf{E}_{\text{ex}}$  on the phase behavior of the TIP4P/2005 water model. Dielectric constants obtained from the linear response region are found to be in good agreement with those obtained from fluctuations. The dielectric constants of ices III, V, and VI are highly anisotropic, but this is not the case for ice Ih. With dipole scaling (correcting for the underestimation of  $\mu$  by the nonpolarizable TIP4P/2005 model), the dielectric constants for the condensed phases are in satisfactory agreement with experiment [10]. For anisotropic crystalline phases, the changes in properties depend on the field direction, and we have focused on  $\mathbf{E}_{\text{ex},\perp,\text{ac}} = 0.3 \text{ V/nm}$  applied in the direction of the largest diagonal element of the dielectric constant tensor. The main result of this work is the prediction that ice II disappears from the phase diagram, ice V increases significantly its region of stability, the melting temperatures of ices III and V increases by about 15 K and the melting point of ice Ih is hardly affected by  $\mathbf{E}_{\text{ex}}$ . Ice III also disappears when the electric field is applied perpendicular to the  $ab$  plane. For fluid phases at  $\mathbf{E}_{\text{ex}} = 0.3 \text{ V/nm}$ , the vapor-liquid coexistence curve is shifted slightly to higher temperatures ( $T_c$  increases by 5 K) and  $T_{\text{md}}$  is shifted downward by the same extent. The structure of cubic ice (Ic) allows for full saturation ( $S_M = 1$ ) [2] and we observe that ice Ic becomes more stable than ice Ih for  $\mathbf{E}_{\text{ex}} > 0.15 \text{ V/nm}$  at low pressure (without dipole scal-

ing) for the TIP4P/2005 model. Thus, a transformation of ice Ih to Ic is not expected at field strength that are experimentally accessible for bulk samples (the dielectric breakdown of bulk water occurs at about  $0.01 \text{ V/nm}$  [1]). The results of this work support the hypotheses that only very small changes in phase transitions should be expected in the experiments, with the exception of the disappearance of ice II which could indeed be experimentally accessible.

Support from grants FIS2010-16159 and FIS2010-22047-C05-05 (DGI), P2009/ESP/1691 (CAM), 910570 (UCM) and CBET-0756641 (NSF) is gratefully acknowledged. J.L.A. would like to thank the MEC for the award of a predoctoral grant and for support of an extended visit to Minnesota, EEBB-2011-43743. Part of the computer resources were provided by the Minnesota Supercomputing Institute.

\*cvega@quim.ucm.es

- [1] C. A. Stan, S. K. Y. Tang, K. J. M. Bishop, and G. M. Whitesides, *J. Phys. Chem. B* **115**, 1089 (2011).
- [2] I. M. Svishchev and P. G. Kusalik, *J. Am. Chem. Soc.* **118**, 649 (1996).
- [3] G. T. Gao, K. T. Oh, and X. C. Zeng, *J. Chem. Phys.* **110**, 2533 (1999).
- [4] K. A. Maerzke and J. I. Siepmann, *J. Phys. Chem. B* **114**, 4261 (2010).
- [5] G. J. Wilson, R. K. Chan, D. W. Davidson, and E. Whalley, *J. Chem. Phys.* **43**, 2384 (1965).
- [6] S. W. Rick and A. D. J. Haymet, *J. Chem. Phys.* **118**, 9291 (2003).
- [7] D. Lu, F. Gygi, and G. Galli, *Phys. Rev. Lett.* **100**, 147601 (2008).
- [8] T. Matsuoka, S. Fujita, S. Shigerari, and S. Mae, *J. Appl. Phys.* **81**, 2344 (1997).
- [9] J. L. F. Abascal and C. Vega, *J. Chem. Phys.* **123**, 234505 (2005).
- [10] J. L. Aragones, L. G. MacDowell, and C. Vega, *J. Phys. Chem. A* **115**, 5745 (2011).
- [11] L. G. MacDowell and C. Vega, *J. Phys. Chem. B* **114**, 6089 (2010).
- [12] A. Rahman and F. H. Stillinger, *J. Chem. Phys.* **57**, 4009 (1972).
- [13] R. A. Alberty, *Pure Appl. Chem.* **73**, 1349 (2001).
- [14] D. Frenkel and B. Smit, *Understanding Molecular Simulation* (Academic Press, London, 2002).
- [15] D. A. Kofke, *J. Chem. Phys.* **98**, 4149 (1993).
- [16] J. F. Nye, *Physical Properties of Crystals* (Oxford University Press, Oxford, 1985).
- [17] S. W. Rick, *J. Chem. Phys.* **122**, 094504 (2005).
- [18] H. E. Alper and R. M. Levy, *J. Chem. Phys.* **91**, 1242 (1989).
- [19] M. Sharma, R. Resta, and R. Car, *Phys. Rev. Lett.* **98**, 247401 (2007).
- [20] E. R. Batista, S. S. Xantheas, and H. Jonsson, *J. Chem. Phys.* **109**, 4546 (1998).
- [21] C. Song and P. Wang, *Rev. Sci. Instrum.* **81**, 054702 (2010).
- [22] A. Z. Panagiotopoulos, *Mol. Phys.* **61**, 813 (1987).